

# Lab on a Chip

Accepted Manuscript



This is an *Accepted Manuscript*, which has been through the Royal Society of Chemistry peer review process and has been accepted for publication.

*Accepted Manuscripts* are published online shortly after acceptance, before technical editing, formatting and proof reading. Using this free service, authors can make their results available to the community, in citable form, before we publish the edited article. We will replace this *Accepted Manuscript* with the edited and formatted *Advance Article* as soon as it is available.

You can find more information about *Accepted Manuscripts* in the [Information for Authors](#).

Please note that technical editing may introduce minor changes to the text and/or graphics, which may alter content. The journal's standard [Terms & Conditions](#) and the [Ethical guidelines](#) still apply. In no event shall the Royal Society of Chemistry be held responsible for any errors or omissions in this *Accepted Manuscript* or any consequences arising from the use of any information it contains.

Cite this: DOI: 10.1039/c0xx00000x

www.rsc.org/xxxxxx

ARTICLE TYPE

## Electro-optical phenomena based on ionic liquids in an optofluidic waveguide

Xiaodong He<sup>a</sup>, Qunfeng Shao<sup>a</sup>, Pengfei Cao<sup>a</sup>, Weijie Kong<sup>a</sup>, Jiqian Sun<sup>a</sup>, Xiaoping Zhang,<sup>\*a</sup> Youquan Deng,<sup>\*b</sup>

Received (in XXX, XXX) Xth XXXXXXXXX 20XX, Accepted Xth XXXXXXXXX 20XX  
DOI:

An optofluidic waveguide with a simple two-terminal electrode geometry, when filled with an ionic liquid (ILs), forms a lateral electric double-layer capacitor under a direct current (DC) electric field, which allows the realization of an extremely high carrier density in the vicinity of the electrode surface and terminals for modulating optical transmission at room temperature under low voltage operation (0 to 4 V). The unique electro-optical phenomenon of ILs was investigated at three wavelengths (663, 1330 and 1530 nm) using two waveguide geometries. The strong electro-optical modulations with different efficiencies were observed at the two near-infrared (NIR) wavelengths, no detectable modulation was observed at 663 nm. The first waveguide geometry was used to investigate the position-dependent modulation along the waveguide, the strongest modulation was observed in the vicinity of the electrode terminal. The modulation phase associates with the applied voltage polarity, which increases in the vicinity of the negative electrode and decreases at the positive electrode. The second waveguide geometry was used to improve the modulation efficiency. Meanwhile, the electro-optical modulations of seven ILs were compared at the applied voltage ranging from  $\pm 2$  V to  $\pm 3.5$  V. The results reveal that the modulation amplitude and response speed increase with increasing applied voltage, as well as the electrical conductivity of ILs. Despite the response speed isn't fast due to the high ionic density of ILs, the modulation amplitude can reach up to 6.0 dB when a higher voltage ( $U = \pm 3.5$  V) is applied for the ILs [Emim][BF<sub>4</sub>]. Finally, the physical explanation of the phenomenon was discussed. The effect of the change of ILs structure to the electro-optical phenomena was investigated with another new experiment. The results reveals that the electro-optical phenomenon is probably caused mainly by the change of carrier concentration (ions redistribution near charged electrodes), which induces the enhancement and suppression of NIR optical absorption (contributed by C-H and N-H groups) in the vicinity of the negative electrode and positive electrode, respectively.

### 1. Introduction

Room-temperature ionic liquids (RTILs or ILs) are low-temperature (by convention below 100 °C) molten organic salts that consist entirely of cations and anions. In contrast to conventional organic liquids/solvents, their properties can be individually customized by rationally modulating the combination of cations and anions.<sup>1</sup> By virtue of their many unique and attractive physicochemical properties (pure liquid electrolytes, high ionic conductivity, wide electrochemical window and vanishingly low vapor pressure), ILs have received increasing attention as a novel class of versatile solvent and functional soft material. In recent years, they have lead innovations in various electroactive devices, including double-layer super capacitors,<sup>2</sup> batteries,<sup>3</sup> dye-sensitized solar cells,<sup>4</sup> electroactive polymer actuators<sup>5, 6</sup> and field-effect transistors.<sup>7, 8</sup> These devices play a dominant role in modern

electronic and materials science fields.

Except the above mentioned applications, electro-optical phenomena provide another fascinating field of ILs electroactive devices. ILs have good transparence in visible light, near-infrared and even in some other infrared regions. The electro-optical devices based on ILs such as electrowetting lens,<sup>9</sup> electrochromic devices,<sup>10, 11</sup> polymeric ionic liquids optical devices<sup>12</sup> and metal organic ionic liquid crystals<sup>13</sup> have been studied widely during the last few years. In addition, very recently, a few of works<sup>14, 15</sup> employed ILs as supporting electrolyte medium in contact with optical film material to increase charge density for achieving electro-optical modulation. Wang *et al.*<sup>14</sup> and Emre *et al.*<sup>15</sup> employed ILs in contact with single-walled carbon nanotube film and grapheme film to achieve optical modulator by controlling interband transitions of these materials, respectively. Despite the growing interest in the properties of ILs electro-optical phenomena, the study of electro-optical phenomena based on ILs is still rather limited. Under application of an external voltage, the

cations and anions of ILs interact with electrode surfaces (redistribution and orientation of ions on the electrode surfaces),<sup>16</sup> such interactions could have an unexpected impact on many physicochemical processes that involve ILs.<sup>17</sup> Furthermore, the molecular dynamics study reveals that the structure of ILs could change from disordered to spatially homogeneous under a strong electric field.<sup>18</sup> However, the effect of ion distribution at electrode surfaces, the change of ions mobility and interionic interaction on their optical properties are remain poorly understood, which limit the application of ionic electroactive optical devices.<sup>6</sup> For this purpose, investigating the electro-optical properties of ILs under an applied voltage is necessary.

Optofluidic technology provides a significant opportunity for fabricating integrated photonic and analytical devices,<sup>19,20</sup> which has been widely used for biological/chemical detection and analysis in the past few years due to its high sensitivity, rapid response and extremely small detection volumes.<sup>21-23</sup> The

optofluidic waveguide merges optical waveguide and fluidic together, which allows the light transmits in the liquids sample. With such waveguide is applied to chemical analysis, the change of sample properties can be very sensitively detected by the optical signal.

In this paper, we propose to use an optofluidic waveguide with electrodes for studying the unique electro-optical phenomena of ILs, where this phenomenon was not observed with some traditional solvents, such as salt solutions (CaCl<sub>2</sub> and NaCl) and organic solutions (ethylene glycol and CCl<sub>4</sub>). We investigated the electro-optical modulation of the ionic liquid [Emim][Nf<sub>2</sub>T] at three wavelengths. The strong modulation was observed at the two near-infrared (NIR) wavelengths (1330 and 1530 nm), and no detectable change in optical power was observed at 663 nm. Firstly, the position-dependent modulation was investigated along the waveguide, the strongest modulation was observed in the vicinity of the electrode terminal. Then, the modulation was

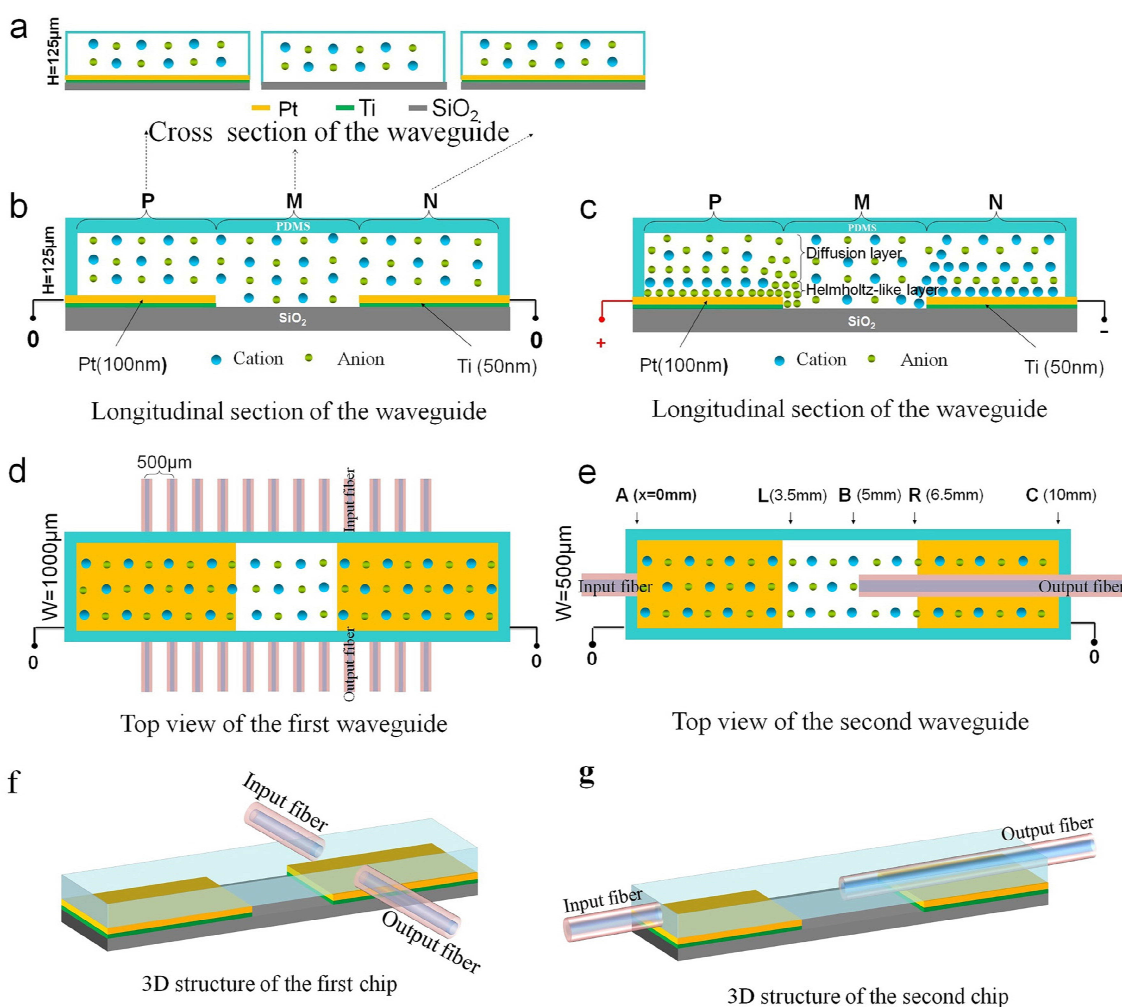


**Fig. 1** Schematic of the set-up for electro-optical measurement with an optofluidic waveguide. (a) Schematic demonstrating the cross section of the waveguide. (b), (c) Schematic demonstrating the longitudinal section of the waveguide and the cations and anions spatial distribution in the waveguide with and without applied voltage. Under a positive applied voltage, anions and cations are redistributed, generating a high concentration of anions in the vicinity of the positive electrode and cations at the negative electrode, forming a lateral electric double-layer capacitor that contains a thin compact layer and a thick diffusion layer. Noted that there is a high ions concentration in the vicinity of the electrode terminals due this region has a very high electric field (see supporting information Fig. S.2). (d), (e) Schematic demonstrating the top view of the two waveguides and the fiber positions, where A,B,C,L and R are the input or output fiber positions we used. (f), (g) Schematic demonstrating the three-dimensional structure of the two waveguides and the fiber positions.

investigated after improving the modulation efficiency with another waveguide; the results reveal that the modulation amplitude, phase and electro-optical response speed associate with the applied voltage (amplitude and polarity). Finally, the electro-optical modulations of seven ILs were compared. The results reveal the modulation amplitude and electro-optical response speed associate with ILs electrical conductivity. Despite the modulation speed is slow (on the order of seconds) due to the very high ionic density of ILs, the modulation amplitude can reach up to 6.0 dB at  $U=\pm 3.5$  V for the high conductivity ionic liquid [Emim][BF<sub>4</sub>]. This phenomenon has potential applications for designing electro-optical devices, such as lab on chip photonic devices (attenuators,<sup>24</sup> switch<sup>25</sup>) and smart windows.<sup>14, 26</sup>

The remainder of this paper is structured as follows: section 2 describes the experimental setup and methods; section 3 gives the measurement results; section 4 study the effect of the change of ILs structure to the electro-optical modulation and discusses the physical explanation of the phenomenon; section 5 provides the conclusions.

## 2. Experimental

### Lateral electric double-layer capacitor

In our waveguide scheme with a two-terminal electrode (Fig. 1), when filled with an ionic liquid, cations and anions interact with charge electrodes, forming a lateral electric double-layer (EDL) capacitor under a direct current (DC) electric field.<sup>16</sup> Understanding of electrical responses of ILs under the operation voltage of electrical devices based on ILs, especially cations and

anions redistribution at electrode surfaces under applied voltage, becomes crucial in guiding the application of ILs and the design of ionic electroactive devices.<sup>6</sup> However, theoretical model of ILs/metal interface is still crudely and sketchy for now, description of anions and cations redistributing near two electrodes is not simple, but relatively complex. To describe the EDL capacitor briefly, we only consider the change of carrier density simply in here, which means there is a high concentration of cations in the vicinity of negative electrode and anions in the vicinity of positive electrode under an applied voltage.<sup>6, 14</sup> For our experimental waveguide, in the presence of the ionic liquid at zero voltage, cations and anions distribute uniformly along the microchannel, as shown schematically in Fig. 1b. With a voltage applied, the anions and cations are redistributed near the two electrodes, forming a lateral EDL capacitor that includes a very thin compact layer and a thick diffusion layer, as shown schematically in Fig. 1c. The inner layer, known as the compact layer or Helmholtz-like layer<sup>16, 27</sup>, which generates a strong electric field intensity and high carrier density at the electrode surfaces due to the thin (a few nanometer) compact layer and extremely large capacitance. The outer element, the diffuse layer is semiinfinite in extent and contains anions and cations distribute unequally, the thickness of diffusion layer depends on voltage and electric field intensity.<sup>28, 29</sup> In addition, the structure of ILs (relative position between the anion and cation will change) under high electric field intensity. Such changes and ions redistribution near the electrode surfaces may have an unexpected impact on its physicochemical properties,<sup>17</sup> including the optical properties.

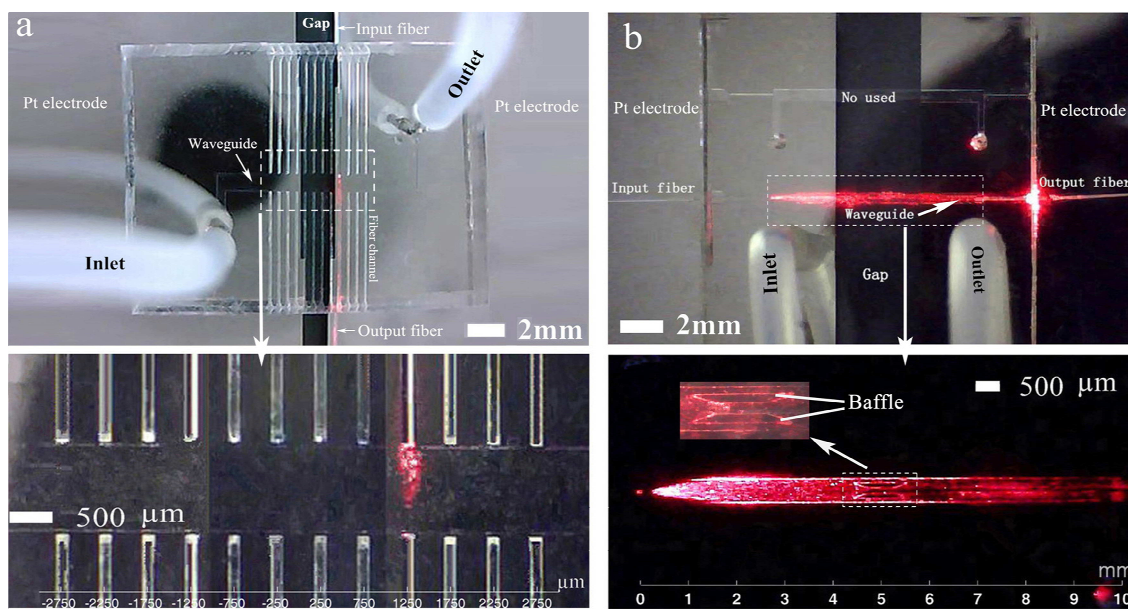


**Fig. 2** The two chips we used in our experiments. **(a)** The first chip working at 663nm wavelength we used. It is used to study the spatial distribution of the electro-optical modulation along the waveguide, it contains a waveguide ( $L=10$  mm,  $W=1$  mm) and 12 pairs fiber input and detector channels ( $W=125$   $\mu$ m), where  $L$  and  $W$  is length and width, respectively. The gap of the two electrodes is 2 mm, the power modulation is investigated every 500  $\mu$ m along the side of the waveguide with 12 pairs fibers. **(b)** The second chip working at 663nm wavelength we used, it contains a waveguide ( $L=10$  mm,  $W=500$   $\mu$ m) and a pairs of input and output fibers channel ( $W=125$   $\mu$ m). The gap of the two electrodes is 4mm. It should be noted that there is a fix baffle at the middle of the microchannel, which can ensure the position of the input and output fiber at the same place every times when we change the sample. The height of all the networks for both chip in this experiment is  $H=125$   $\mu$ m.

**Table 1**  
The details of the chemicals used.

Chemical name	Source	Purification method	Purity (mass%)	Analysis method
[Emim][Nf <sub>2</sub> T]	Synthesized in our lab: Lanzhou Institute of Chemical Physics, Chinese Academy of Sciences., China	Dissolving IL in dichloromethane; removing salts by washing IL 5 times with deionized water; distilling dichloromethane; removing water by drying in vacuum.	>0.99	<sup>1</sup> H NMR <sup>a</sup> , Br contents <sup>b</sup> , Water content <sup>c</sup>
[Bmim][Nf <sub>2</sub> T]			>0.99	
[Emim][BF <sub>4</sub> ]			>0.99	
[Bmim][BF <sub>4</sub> ]			>0.99	
[Bmim][PF <sub>6</sub> ]			>0.99	
[Bmim][ClO <sub>4</sub> ]			>0.99	
[Emim][N(CN) <sub>2</sub> ]			>0.99	

<sup>a</sup> The data of <sup>1</sup>H NMR is listed in the supplementary material.

<sup>b</sup> The Br contents of all the ILs are lower than 0.1 wt.-%.

<sup>c</sup> The Water contents of all the ILs are lower than 500 ppm.

Note that the physical explanation of the electro-optical phenomenon in such lateral EDL capacitor is detailed described in section 4.

### Device fabrication

The optofluidic waveguide chip consists of two layer structures. One is the top sealing layer and another is the bottom electrode layer (Fig. 1f and 1g). The top part is a polydimethylsiloxane (PDMS) piece that contains a network of microchannels. The microchannels were fabricated by the standard soft lithography processes using the most popular polymer, PDMS, due to its advantages in electrical properties (breakdown voltage,  $2 \times 10^7$  V/m), chemical properties (unreactive toward ILs) and surface properties (smooth on the micron scale). The PDMS has a refractive index around  $n=1.41$ . The bottom layer is a smooth glass slide with electrode patterned. The metal platinum (Pt) electrode is commonly used in ILs, because it is stable enough in an ionic liquid electric double layers experiment. In here, the Pt electrode patterned was produced using photolithography, physical sputtering, and lift-off of photoresist. The electrode layer is a smooth glass slide electrode patterned with a 50 nm thick titanium (Ti) layer acting as adhesion layer and a 100 nm thick Pt layer. Finally, the PDMS top layer and the SiO<sub>2</sub> substrate with pattern electrodes were conformally bonded to each other by aligning the electrodes with the PDMS channels under a microscope. The two chips are shown in Fig. 2. The fabrication of the micro-channels and microelectrodes is described in the supplementary materials. In addition, the indium–tin oxide (ITO) and Cuprum (Cu) electrodes were also studied in our experiment, but they are not suit for our experiment due to the narrow electrochemical window in ILs and the low modulation

efficiency.

### Experimental setup for measurement

The experimental system is shown schematically in Fig. 3. Firstly, an ionic liquid sample was placed in a syringe, and promptly added to the microchannel. Then, the input and output fibers were inserted into the two fiber pre-fabricated microchannels with a width of 125 μm. Light from laser source ( $\lambda=663, 1330$  and 1530 nm) was coupled into the chip using the input Multimode optical fiber (cladding diameter: 125 μm, core diameter: 62.5 μm) with a numerical aperture of 0.22. The output fiber was connected with an Optical Spectrum Analyzer (China, CETC, AV6362) to record the time-dependent optical peak powers under applied voltage. It should be noted that the modulation amplitude is sensitive to the position of the input and output fiber. To avoid the error caused by the variance of fiber position in the experiments, we used a fix baffle for the second waveguide to enable the comparison of modulation realized under the same condition. In addition, because most of ILs are mutually soluble, the sample can be easily washed away and substituted with another ionic liquid, which allowed us to investigate the modulation of different ILs under the same condition.

In our experiment, a DC voltage was applied cyclically with a period of 90 or 60 seconds. All of the experiments were repeated several times to ensure the reproducibility of the data, as it is necessary to obtain reversible and reproducible results. The ionic liquid and electrode will occur chemical reactions when the modulation voltage equal or slightly larger limited gate voltage, which would result in irreversible device degradation, the modulator will die within a few minutes. Therefore, the measurements were performed in a limited gate voltage range, to avoid the occurrence of chemical reactions between the electrode and ILs. In addition, because of the sensitivity of ILs to moisture (humidity present in ILs can significantly increase the tendency to chemical reactions when the voltage is applied), as well as the water would undoubtedly lead to changes in the optical absorption characteristic due to the O-H group of water, the chip was left under vacuum oven for several hours before starting the measurements. All of the experiments were done at room temperature (25 °C) for minimizing experiment errors.

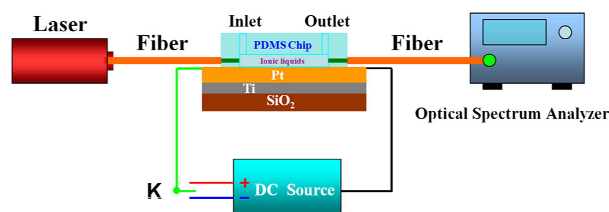


**Fig. 3** Experiment system schematic of electro-optical modulation with an optofluidic waveguide chip.

### 70 Ionic liquids Synthesis and Preparation

ILs based on the 1, 3-methylimidazolium cation have generated a great deal of interest over the past few years as solvents in many different areas of chemistry due to their ease of preparation. In our experiment, seven 1, 3-methylimidazolium ILs e.g., [Emim][BF<sub>4</sub>], [Bmim][BF<sub>4</sub>], [Emim][Nf<sub>2</sub>T], [Bmim][Nf<sub>2</sub>T], [Bmim][ClO<sub>4</sub>], [Emim][N(CN)<sub>2</sub>] and [Bmim][PF<sub>6</sub>] were synthesized according to the literature method in subsequent studies.<sup>30, 31</sup> The structures of the seven ionic liquids are shown in Fig. S1. It is crucial to ensure the purity of ILs since their properties could be affected greatly by contaminants. These ILs were dried under vacuum at 70 °C for 4 hours and kept them under a vacuum desiccator to protect them from moisture. For each IL, the <sup>1</sup>H NMR spectrum contains peaks corresponding to their cation and indicates no residual reactants. The Br contents and water contents of all the ILs are lower than 0.1 wt.-% and 500 ppm, respectively. The source, purification method and purity of the chemicals are reported in supplement material Table 1. In general, ILs used in our study are high purity, transparent and with a vanishingly low amount of water.

### 3. Experimental results

We used two waveguide chips with electrodes to study the electro-optical phenomena. The first chip is used to study the spatial distribution of the electro-optical modulation along the waveguide, as shown in Fig. 2a. The second chip is used to improve the modulation efficiency by increasing the length of modulation region, as shown in Fig. 2b. For different refractive index ILs waveguides, the light output power and transmission efficiency are different. To evaluate the electric-optical modulation efficiency of different ILs, we defined the normalized peak power of optical signal  $N_p = P(U)/P_{U=0}$ , where  $P_{U=0}$  is the peak power in the absence of an applied voltage (at  $U=0$  V),  $P(U)$  is the peak power with the application of a voltage. With the normalized method was used to calculate the relative change of optical power under an applied voltage, the effect of refractive index of different ILs to modulation efficiency can be eliminated.

We used 12 pairs input and output fibers at the side of the waveguide (Fig. 1d and Fig. 2a) to study the spatial distribution of optical modulation along the waveguide at the applied voltage

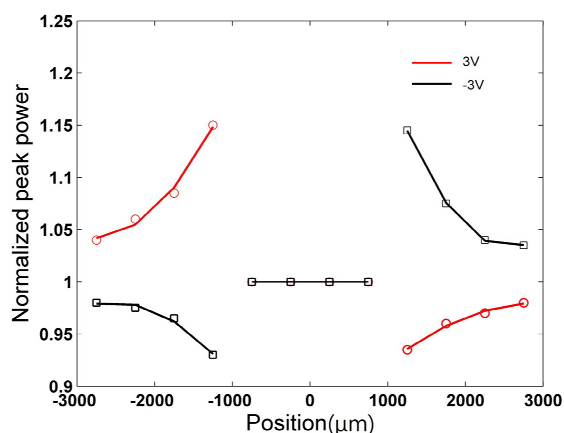


Fig. 4 Spatial distribution of the electro-optical modulation along the first waveguide.

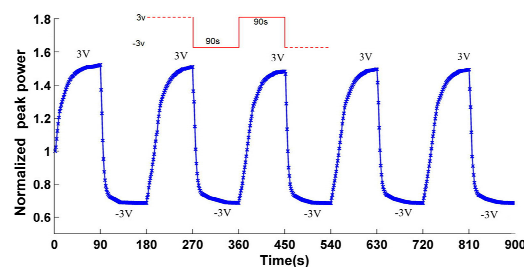
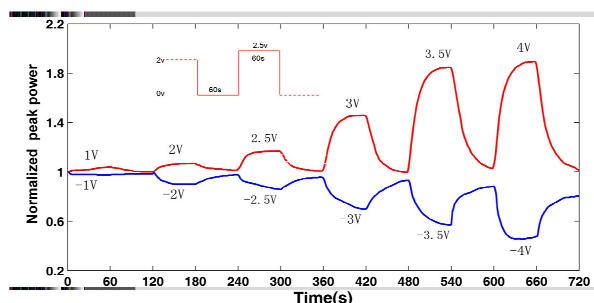


Fig. 5 Temporal response of electro-optical modulation for [Emim][Nf<sub>2</sub>T] at  $\lambda=1530$ nm.

of 3V and -3V. The microchannel is filled with the ionic liquid [Emim][Nf<sub>2</sub>T]. The optical peak power was recorded after 60s under the applied voltage. The modulation results are shown in Fig. 4, it is found that the optical normalized peak power increases in the positive electrode and decreases in the negative electrode. It should be noted that the modulation amplitude is different at different positions, the modulation was observed at the two electrodes region (P section and N section) and no detectable electro-optical modulation was observed in the middle region (M section: without electrode). Meanwhile, the strongest modulation was observed in the vicinity of the two electrode terminals ( $x=\pm 1250$  μm), which is likely due to the nonuniform electric field intensity in the waveguide. To substantiate our speculation, the distribution of electric field intensity in the waveguide is simulated with commercial software COMSOL Multiphysics 4.3a. Under an applied voltage, the high electric field region is generated in the vicinity of the two electrode terminals due to the very thin electrode, even the EDL effect is not considered. The electric field intensity at the terminal is much higher than other positions of the two electrodes, as shown in Fig. S.2 (supporting information).

However, the modulation efficiency is quite low with the first geometry chip. To improve the electro-optical modulation efficiency, we increase the length of modulation region and let the light transmission through the highest electric field intensity region (near position L or R) using the second waveguide chip (Fig. 2b), as shown schematically in Fig. 1e. The input fiber was fixed at position A and the output fiber was fixed at position B. The microchannel was filled with the ionic liquid [Emim][Nf<sub>2</sub>T], a voltage square waveform of 3V to -3V and of 90 seconds cyclically period was applied. The peak power was recorded every 1.5 seconds. Fig. 5 shows the normalized peak power as a function of the polarity of the applied voltage at a fixed wavelength of 1530 nm. With the application of a positives voltage, the normalized peak power increases slowly and then reaches to a constant value. With the application of a negative voltage, the normalized peak power decreases quickly and then reaches to a constant value. The asymmetric electro-optical response speed and modulation amplitude between the two polarities of the applied voltage are likely associated with the properties of the ionic liquid, and in large part caused by the large difference in ion size and mobility between cations and anions.



**Fig. 6** Temporal response of electro-optical modulation of ionic liquid [Emim][Nf<sub>2</sub>T] at 1530 nm as a function of the amplitude and polarity of the applied voltage.

In Fig. 6, we studied the normalized peak power as a function of amplitude and the polarity of the applied voltage at a fixed wavelength of 1530 nm. The voltage increases from 1V to 4.5V and -1V to -4.5V, the cyclically period is 120 seconds (60s applied voltage and 60s zero voltage). As shown in Fig. 5, the modulation amplitude increases with the application voltage. It should be noted that the modulation amplitude isn't linearly increase. There is only a slight optical peak power modulation at lower applied voltage ( $U < 2$  V). With further increase of voltage, the modulation amplitude increases strongly. While application of a high voltage ( $U = \pm 4$  V), it shows a rather large modulation amplitude ( $N_p$  from 0.45 to 1.89) and expands as higher as 6.2 dB. However, it should be noted that the modulation amplified increases slowly and reaches to a constant value when the applied voltage near to the electrochemical window ([Emim][Nf<sub>2</sub>T]:4.3 V, working electrode: Pt).

To substantiate all the considerations, other two situations of input-output fiber positions were investigated at a fixed wavelength 1530 nm. One is the input-output fiber at position B-C, and another is the input-output fiber at position L-R (L:

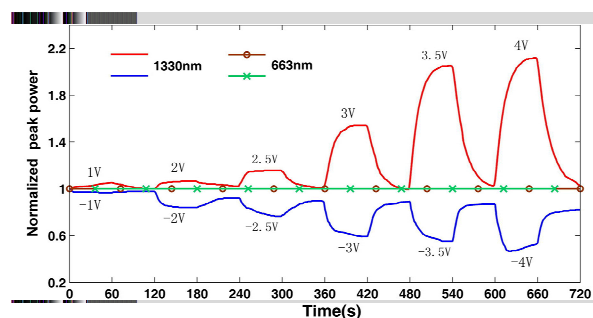


**Fig. 7** Temporal response of electro-optical modulation for ionic liquid [Emim][Nf<sub>2</sub>T] at  $\lambda=1330$  nm and  $\lambda=663$  nm as a function of the amplitude and polarity of the applied voltage.

$x=3.5$  mm and R:  $x=6.5$  mm, in Fig. 1e). Compared with the results (Fig. 5) of the situation A-B, the modulation phase of the first situation (B-C) is inverse at the same applied voltage polarity. With a positive voltage and a negative voltage is applied, the normalized peak power decreases and increases, respectively. For the second situation (at the M section), no modulation was observed.

In Fig. 7, we investigated the normalization peak power as a function of amplitude and the polarity of the applied voltage at a fixed wavelength of 1330 and 663 nm under identical conditions with Fig. 6. The peak power was recorded every 1.5 seconds. As shown in Fig. 7, the results shows the similar modulation behaviours at 1330 nm compare with at 1530 nm (Fig. 6), but the modulation amplitude has a slight difference for each other. Meanwhile, no change in the optical peak power was observed under an applied voltage at 663 nm.

In order to reveal the inherent law of ILs photoelectric characteristic as far as possible, the electric-optical modulation was studied for different ILs under the identical condition. We studied the electric-optical phenomenon with seven different

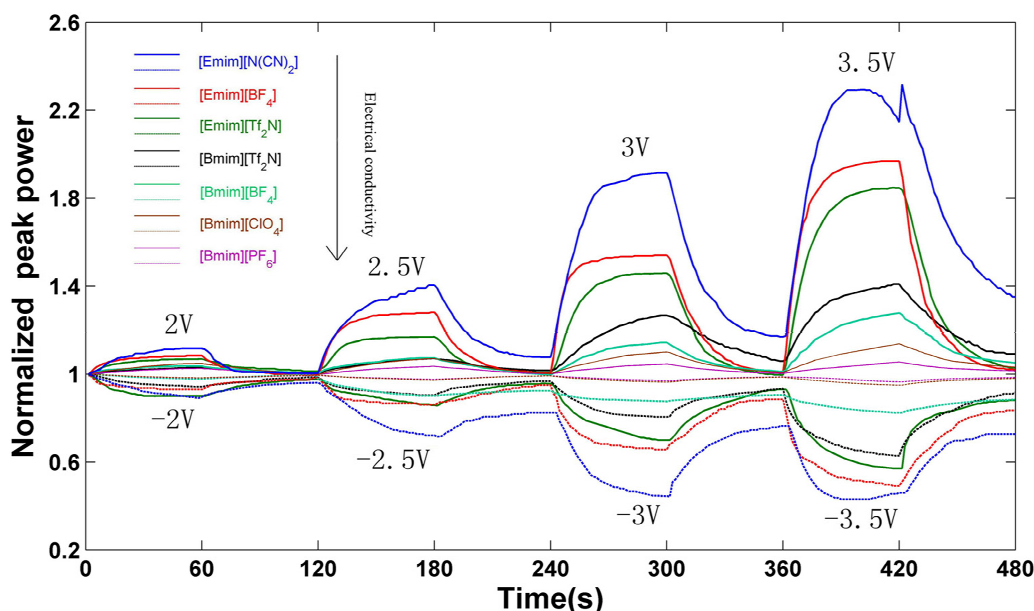


**Fig. 8** Temporal response of electro-optical modulation for seven ionic liquids at wavelength  $\lambda=1530$  nm.

**Table 2**

Refractive index  $n$ , electrochemical window  $U_w$  (working electrode: Pt), dynamic viscosity  $\mu$ , electrical conductivity  $\epsilon$  and the electrical modulation respond time ( $T_s$ ) of seven different ionic liquids at 298.2K and atmospheric pressure.

RTILs	$n$	$U_w$ (V)	$\mu$ (mPa·s)	$\epsilon$ (mS·cm <sup>-1</sup> )	$T_s$ (s)	
					+1dB	-1dB
[Emim][Nf <sub>2</sub> T]	1.4231	4.3	26.1	9.20	10.5	9
[Bmim][Nf <sub>2</sub> T]	1.4269	4.7	50.0	4.08	52.5	60
[Emim][BF <sub>4</sub> ]	1.4142	4.8	36.9	16.3	4.5	7.5
[Bmim][BF <sub>4</sub> ]	1.4219	4.6	112.0	3.52	>60	>60
[Bmim][ClO <sub>4</sub> ]	1.4736	3.6	180.3	1.80	-	-
[Bmim][PF <sub>6</sub> ]	1.4101	4.6	273.0	1.49	-	-
[Emim][N(CN) <sub>2</sub> ]	1.5130	3.3	14.9	29.3	3.0	4.5

<sup>a</sup> the optical peak power can't increase or decrease 1 dB at  $U=\pm 3$  V, due to their low electrical conductivity and high viscosity.

Standard uncertainties  $u$  for refractive index, temperature, dynamic viscosity, and electrical conductivity are  $u(n)=0.0001$   $u(T)=0.1$ K;  $u(\mu)=0.5$ mPa·s;  $u(T_s)=0.5$ s and  $u(\epsilon)=0.01$ mS·cm<sup>-1</sup>, respectively

imidazolium-based ILs: [Emim][Nf<sub>2</sub>T], [Bmim][Nf<sub>2</sub>T], [Bmim][BF<sub>4</sub>], [Emim][BF<sub>4</sub>], [Bmim][ClO<sub>4</sub>], [Bmim][PF<sub>6</sub>] and [Emim][N(CN)<sub>2</sub>], the two fibers at position (A-B). The date of the refractive index, electrochemical window (working electrode: Pt), dynamic viscosity and electrical conductivity of these seven different ILs are listed in Table 2. Fig. 8 shows the temporal response of electro-optical modulation as a function of the amplitude and polarity of the applied voltage from  $\pm 2$  to  $\pm 3.5$  V at 1530 nm. Meanwhile, the electro-optical response times of optical peak power increases 1 dB ( $N_p=1.26$ ) and decreases 1 dB ( $N_p=0.79$ ) are also analyzed in Table. 2 at applied voltage  $U=\pm 3$  V. The relationship of modulation efficient with ILs viscosity and electrical conductivity is also analyzed in Table. 2. Our results reveal that the modulation amplitude and electrical-optical response speed decrease with ILs electrical conductivity. It is likely that the low electrical conductivity and high ionic density of ILs cause the restructuring is kinetically slow. Despite that, the modulation amplitude efficiency can reach up to 6.0 dB ( $N_p$  from 0.49 to 1.97) when a higher voltage ( $U=3.5$  V) is applied for the ionic liquid [Emim][BF<sub>4</sub>]. It should be noted that the modulation amplitude does not monotonous increase with the modulation voltage, but has a peak value. The high voltage (applied voltage equal or slightly larger than the electrochemical window) led to a decrease of the modulation amplitude (as shown in Fig. 7 for [Emim][N(CN)<sub>2</sub>]), because the modulator occurs chemical reactions.

Our results reveal that the NIR optical power have a suppression of in the vicinity of the negative electrode (P section in Fig. 1c) and an enhancement in the vicinity of positive electrode (N section in Fig. 1c) under an applied voltage, and as a result, generating the electro-optical phenomenon in the lateral EDL capacitor. The electrical control of the NIR optical transmission suggests applications of ionic liquids as electrochromic materials (materials that can change their optical properties under an applied voltage) for engineering electrochromic smart windows. In addition, this phenomenon also has potential applications for fabricating electro-control optofluidic devices, such as attenuators and switch.

#### 4. The physical explanation of the phenomenon

At this stage, detailed mechanism of modulation is still not entirely clear because of the very complex structure of ILs in the vicinity of the electrode surface. From the results obtained, we conjecture that the electro-optical phenomenon may be caused by the change of carrier concentration and ions redistribution. Under an applied voltage, mobile ions will redistribute in the vicinity of the electrode surfaces due the thin EDL and the strong electric field intensity, generating a high concentration of cations than anions and anions than cations at the negative electrode surface and the positive electrode surface, respectively. Since the cations of imidazolium ILs possess at least one or more of C-H and N-H groups, those groups stretching vibrations like N-H or C-H and their overtone and combination transitions contribute to radiationless deactivation or absorption at NIR wavelength.<sup>32, 33</sup> Therefore, the excess cations than anions in the vicinity the negative electrode leads to the enhancement and less cations than anions at positive electrode leads to suppression of NIR optical absorption.

In addition, the results reveal that the strong electro-optical modulations were observed at the two near-infrared (NIR) wavelengths and no detectable modulation was observed at 663 nm, which indicates that the modulation could not be caused by the change of ILs refractive index.

According to the above speculation, that could be explained why no modulation was observed in M section (in Fig. 4), it may be because the distribution of cations and anions is uniform in this region even an external voltage is applied. In addition, the strongest modulation was observed in the region of the highest electric field intensity, which can be explained that this region has a higher ions concentration. Moreover, the modulation efficiency of the ionic liquid [Emim][Nf<sub>2</sub>T] is different at different wavelengths (Fig. 6 and Fig. 7). It could be because the main absorption of 1, 3-methylimidazolium ILs is contributed by the 1<sup>st</sup> overtone of C-H combinations at 1330 nm and contributed by N-H 1<sup>st</sup> overtone at 1530 nm, and the ionic liquid [Emim][Nf<sub>2</sub>T] nearly doesn't absorb light at 663 nm. In other word, the difference of optical absorption features result in the modulation efficiency is different at different wavelengths.

As is well known, ILs absorption characteristics are attributed to the imidazolium moiety and its various associated structures<sup>34</sup>. The anionic component plays a key role in the association of the



cationic components (the imidazolium ions) and indirectly influences the optical properties of ILs. Therefore, the change of ILs structure (relative position between the anion and cation) also affect the optical properties under an external electric field. In here, the effect of the change of relative position to the electro-optical phenomena was investigated with another experiment (see supporting information Fig. S.4). The results reveal that **the change of relative position between the anion and cation can contribute to the electro-optical modulation only under a very strong external electric field** (see supporting information Fig. S.5). The contribution of the change of relative position between the anion and cation to the electro-optical modulation is very small when the external electric field is not very strong (less than 100000 V/m). In the lateral EDL capacitor geometries, the electric field intensity could not very strong due to the low applied voltage. In addition, the two electro-optical modulations have a large difference in the response speeds (see supporting information Fig. S.6). Therefore, we conclude that **the modulation in the lateral EDL capacitor geometries is probably caused mainly by the change of carrier concentration**.

## 5. Conclusions

**In this paper, we designed a small lateral EDL capacitor in an optofluidic chip and reported the unique electro-optical phenomena of ILs with it**, where this phenomenon was not observed with some traditional solvents. **The strong modulation of the optical power was observed at the 1530 nm and 1330 nm NIR wavelengths. The electro-optical modulation amplitude and response speed associate with the applied voltage and amplitude and modulation wavelength, and the modulation phase can be controlled by the applied voltage polarity.** Meanwhile, the modulation amplitude and electro-optical response speed also associate with electrical conductivity of ILs. In addition, we also observed the electro-optical phenomena caused by the change of ILs structures under strong external static electric field. Our studies indicate that the modulation in the lateral EDL capacitor is caused mainly by anions and cations redistribution. We believe that the two electro-optical phenomena we observed could be used in some optical applications. **ILs could be used as a novel class of soft material for creating electrically tunable optofluidic devices.**

## Acknowledgments

This work was supported by the National Natural Science Foundation of China (No. 21373247 and No. 61205204) and the Fundamental Research Funds for the Central Universities (lzujbky-2014-46, lzujbky-2014-44 and lzujbky-2014-236).

## Notes and References

<sup>a</sup> School of Information Science and Engineering, Lanzhou University, No.222 Tianshui South Road, Lanzhou 730000, China. E-mail: zxp@lzu.edu.cn

<sup>b</sup> Centre for Green Chemistry and Catalysis, Lanzhou Institute of Chemical Physics, Chinese Academy of Sciences, No.18 Tianshui Middle Road, Lanzhou, 730000, China. E-mail: ydeng@licp.cas.cn

† Electronic Supplementary Information (ESI) available: [details of any supplementary information available should be included here]. See DOI:

- M. Armand, F. Endres, D. R. MacFarlane, H. Ohno and B. Scrosati, *Nature materials*, 2009, **8**, 621-629.
- M. Ue, M. Takeda, A. Toriumi, A. Kominato, R. Hagiwara and Y. Ito, *Journal of the Electrochemical Society*, 2003, **150**, A499-A502.
- T. Kuboki, T. Okuyama, T. Ohsaki and N. Takami, *Journal of Power Sources*, 2005, **146**, 766-769.
- P. Wang, S. M. Zakeeruddin, J.-E. Moser and M. Grätzel, *The Journal of Physical Chemistry B*, 2003, **107**, 13280-13285.
- D. Zhou, G. M. Spinks, G. G. Wallace, C. Tiyapiboonchaiya, D. R. MacFarlane, M. Forsyth and J. Sun, *Electrochimica Acta*, 2003, **48**, 2355-2359.
- Y. Liu, C. Lu, S. Twigg, M. Ghaffari, J. Lin, N. Winograd and Q. Zhang, *Scientific reports*, 2013, **3**.
- S. Ono, S. Seki, R. Hirahara, Y. Tominari and J. Takeya, *Applied Physics Letters*, 2008, **92**, 103313.
- J. Ye, M. F. Craciun, M. Koshino, S. Russo, S. Inoue, H. Yuan, H. Shimotani, A. F. Morpurgo and Y. Iwasa, *Proceedings of the National Academy of Sciences*, 2011, **108**, 13002-13006.
- X. Hu, S. Zhang, C. Qu, Q. Zhang, L. Lu, X. Ma, X. Zhang and Y. Deng, *Soft Matter*, 2011, **7**, 5941-5943.
- W. Lu, A. G. Fadeev, B. Qi, E. Smela, B. R. Mattes, J. Ding, G. M. Spinks, J. Mazurkiewicz, D. Zhou and G. G. Wallace, *Science*, 2002, **297**, 983-987.
- T. Sato, G. Masuda and K. Takagi, *Electrochimica Acta*, 2004, **49**, 3603-3611.
- J. Huang, C.-a. Tao, Q. An, W. Zhang, Y. Wu, X. Li, D. Shen and G. Li, *Chem. Commun.*, 2010, **46**, 967-969.
- G. V. Klimusheva, A. V. Koval'chuk, N. Volynets and A. Y. Vakhnin, Electro-optical properties of metal organic ionic liquid crystals, 2002.
- F. Wang, M. E. Itkis, E. Bekyarova and R. C. Haddon, *Nature Photonics*, 2013, **7**, 459-465.
- E. O. Polat and C. Kocabas, *Nano letters*, 2013, **13**, 5851-5857.
- S. Baldelli, *Accounts of chemical research*, 2008, **41**, 421-431.
- Y. Z. Su, Y. C. Fu, J. W. Yan, Z. B. Chen and B. W. Mao, *Angewandte Chemie*, 2009, **121**, 5250-5253.
- Y. Wang, *The Journal of Physical Chemistry B*, 2009, **113**, 11058-11060.
- C. Monat, P. Domachuk and B. Eggleton, *Nature Photonics*, 2007, **1**, 106-114.
- L. Pang, H. M. Chen, L. M. Freeman and Y. Fainman, *Lab on a Chip*, 2012, **12**, 3543-3551.
- X. He, Q. Shao, W. Kong, L. Yu, X. Zhang and Y. Deng, *Fluid Phase Equilibria*, 2014, **366**, 9-15.
- N. Dossi, R. Toniolo, A. Pizzariello, E. Carrilho, E. Piccin, S. Battiston and G. Bontempelli, *Lab on a Chip*, 2012, **12**, 153-158.
- W. Song and J. Yang, *Lab on a Chip*, 2012, **12**, 1251-1254.
- A. J. Chung and D. Erickson, *Optics express*, 2011, **19**, 8602-8609.
- J.-M. Lim, J. P. Urbanski, T. Thorsen and S.-M. Yang, *Applied Physics Letters*, 2011, **98**, 044101.
- R. Baetens, B. P. Jelle and A. Gustavsen, *Solar Energy Materials and Solar Cells*, 2010, **94**, 87-105.
- J. Wu, T. Jiang, D.-e. Jiang, Z. Jin and D. Henderson, *Soft Matter*, 2011, **7**, 11222-11231.
- K. B. Oldham, *Journal of Electroanalytical Chemistry*, 2008, **613**, 131-138.
- A. A. Kornyshev, *The Journal of Physical Chemistry B*, 2007, **111**, 5545-5557.
- P. Bonhote, A.-P. Dias, N. Papageorgiou, K. Kalyanasundaram and M. Grätzel, *Inorganic chemistry*, 1996, **35**, 1168-1178.
- J. G. Huddleston, A. E. Visser, W. M. Reichert, H. D. Willauer, G. A. Broker and R. D. Rogers, *Green chemistry*, 2001, **3**, 156-164.
- C. D. Tran, S. H. De Paoli Lacerda and D. Oliveira, *Applied spectroscopy*, 2003, **57**, 152-157.
- A. Dominguez-Vidal, N. Kaun, M. J. Ayora-Cañada and B. Lendl, *The Journal of Physical Chemistry B*, 2007, **111**, 4446-4452.
- A. Paul and A. Samanta, Optical absorption and fluorescence studies on imidazolium ionic liquids comprising the bis (trifluoromethanesulphonyl) imide anion, 2006.